6620–6632 *Nucleic Acids Research, 2008, Vol. 36, No. 20* *Published online 21 October 2008*
doi:10.1093/nar/gkn669

Novel mechanism of hexamer ring assembly in protein/RNA interactions revealed by single molecule imaging

Feng Xiao, Hui Zhang and Peixuan Guo*

Department of Biomedical Engineering, College of Engineering/College of Medicine, University of Cincinnati, Cincinnati, OH 45221, USA

Received June 26, 2008; Revised and Accepted September 22, 2008

ABSTRACT

Many nucleic acid-binding proteins and the AAA+ family form hexameric rings, but the mechanism of hexamer assembly is unclear. It is generally believed that the specificity in protein/RNA interaction relies on molecular contact through a surface charge or 3D structure matching via conformational capture or induced fit. The pRNA of bacteriophage phi29 DNA-packaging motor also forms a ring, but whether the pRNA ring is a hexamer or a pentamer is under debate. Here, single molecule studies elucidated a mechanism suggesting the specificity and affinity in protein/RNA interaction relies on pRNA static ring formation. A combined pRNA ring-forming group was very specific for motor binding, but the isolated individual members of the ring-forming group bind to the motor nonspecifically. pRNA did not form a ring prior to motor binding. Only those RNAs that formed a static ring, via the interlocking loops, stayed on the motor. Single interlocking loop interruption resulted in pRNA detachment. Extension or reduction of the ring circumference failed in motor binding. This new mechanism was tested by redesigning two artificial RNAs that formed hexamer and packaged DNA. The results confirmed the stoichiometry of pRNA on the motor was the common multiple of two and three, thus, a hexamer.

INTRODUCTION

A variety of DNA and RNA metabolic processes essential to normal cell functioning, such as replication, recombination, repair and translation, involve molecular motors which use the energy derived from nucleotide hydrolysis to unwind or translocate the nucleic acid structure. The formation of a hexameric ring appears to be common for components or enzymes of the DNA or RNA processing machinery. This class includes DNA helicases (1,2), RNA packaging motor (3), transcription termination factor Rho (4,5), DNA polymerases and replication factors (6), SV40 large T antigen (7), the DNA replication sliding clamp (8), RNA polymerase (9), and members of the AAA+ family of ATPases (10–14). While the primary sequence conserved within a class of enzymes may dictate the specific biological task to be performed, the structural arrangement into a hexameric ring may reflect an evolutionary link among enzymes required to move with high fidelity and processivity along nucleic acid strands. The geometrical constraints imposed by a hexameric ring structure may be reflected in optimal molecular contacts with other interacting proteins or nucleic acids and high binding affinities. Besides the DNA or RNA processing machineries, formation of the hexameric complexes have also been found in many other proteins. Why nature creates such an elegant ring structure remains to be further elucidated.

Small RNA species have emerged to play a critical role in regulating a variety of diverse biological activities. Protein/RNA interaction is an intriguing subject of scrutiny. The flexibility and versatility in RNA structure led to its impressive functional diversity (15–17). It is interesting to find that RNA molecules, which are composed of only four nucleotides, exhibit versatile novel functions. The enzymatic roles played by some of the RNA molecules have been elucidated (18–20). The secondary RNA structure is governed by the primary sequence. It is generally believed that the specificity in protein/RNA interaction relies on the molecular contacts, via surface charge attraction or 3D structural matching. Models such as Key and Lock, Conformational Capture, and Induced Fit have also been proposed (21,22). Nevertheless, these models or theories still require a specific RNA sequence for protein/RNA contact. In this article, we report on a new mechanism of specific protein/RNA interaction that relies on RNA static ring formation.

During the last step of replication, dsDNA viruses package their genomic DNA into a limited space inside

*To whom correspondence should be addressed. Tel: +1 513 558 0041; Fax: +1 513 558 6079; Email: guopn@ucmail.uc.edu

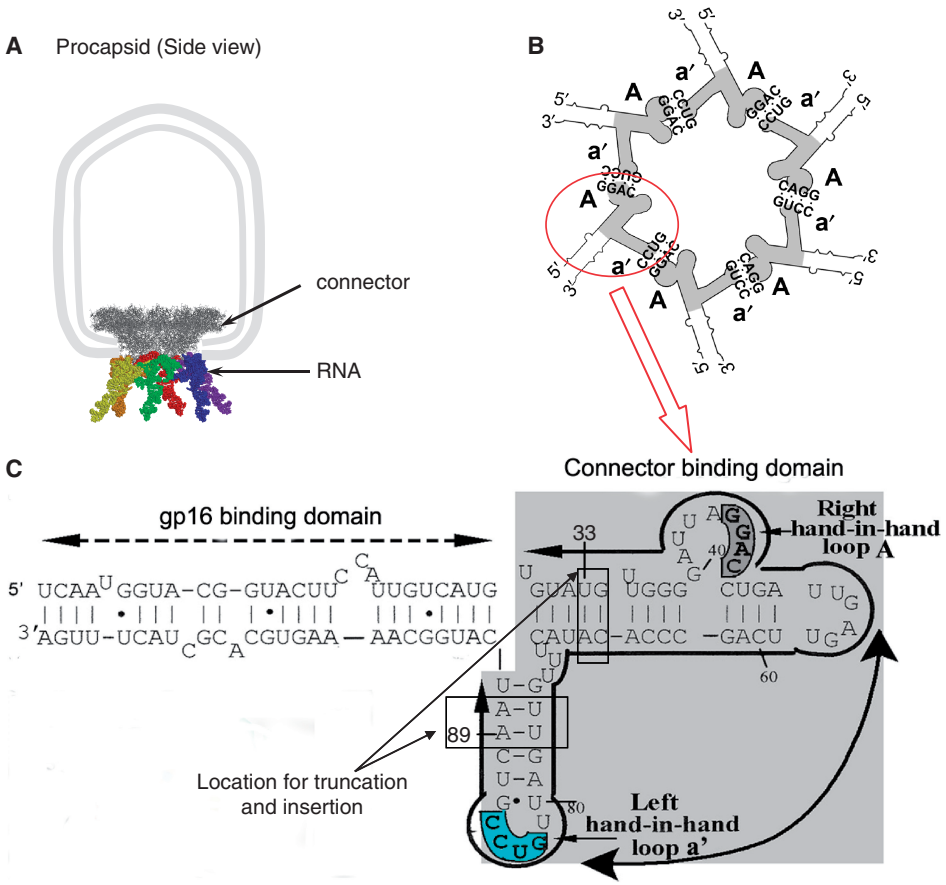

Figure 1. Secondary structure of pRNA and hexamer formation. (**A**) Side-view of phi29 procapsid. (**B**) Illustration of right- and left-hand interaction via the interlocking right loop A (5′GGAC) and left loop a′ (3′CCUG) to form a pRNA hexamer. The connector binding domain is shaded. (**C**) Sequence and secondary structure of pRNA Aa′. The lightly boxed regions indicate the location for the truncation and insertion of nucleotide to construct mutant pRNAs that form into pRNA hexameric rings with reduced or enlarged diameter, respectively.

the procapsid (a preformed protein shell) (23–28). This entropically unfavorable DNA translocation task is accomplished by a DNA packaging motor that includes a portal protein called the connector (29–33). ATP hydrolysis provides the energy for DNA translocation (34–41). In bacteriophage phi29, the motor is geared by six pRNAs (packaging RNA) (42–44). Phi29 pRNA contains two functional domains [for review, see (45); Figure 1C]. The 5′/3′ paired helical domain is for binding of a DNA-packaging ATPase gp16 (46); while, the connector binding domain is located at the central region (47,48). Computer models of the 3D structure of pRNA monomer, dimer and hexamer have been constructed (48) based on various experiments, such as photoaffinity cross-linking (49), chemical modification interference (50,51), complementary modification (52), nuclease probing (47,53), competition assays (54) and cryo-atomic force microscopy (50,51,55). The connector binding domain of the pRNA governs the size and shape of the pRNA ring, which is formed via a hand-in-hand interaction through the base pairing of two interlocking left- and right-hand loops (56–59) (Figure 1A and B). These loops dictate the formation of dimeric, trimeric and hexameric rings. In the pRNA hexamer, this domain also determines the diameter of the central channel to be ~7.6 nm (48). It has been confirmed that phi29 pRNA binds to the first 14 amino acids at the N-terminus of connector protein gp10 (53,60,61), the subunit of the dodecameric ring structure. A comprehensive evaluation in combination with the finding that the activity of the combined pRNA ring forming group is very specific in DNA packaging (56,59,62–64) has led to the speculation that a specific pRNA sequence or conformation is required for pRNA and gp10 or connector interaction. Although the arginine or lysine-rich N-terminus of gp10 has a tendency to bind the pRNA; here, we report an unexpected finding that connector binds to diverse RNA or DNA such as tRNA, DNA oligos or the isolated individual pRNA subunit with similar affinity. That is, the isolated individual pRNA subunit binds to the motor, connector or procapsid nonspecifically. However, only those RNAs which are capable of forming a static ring via the interlocking loops can stay on the procapsid.

The novelty of RNA molecules to gear viral DNA-packaging motor has attracted great attention to scientists in biophysics, virology, phage biology, RNA chemistry, molecular biology, energy transduction, nanotechnology and many other fields. However, there were discrepancies and keen debate regarding whether the pRNA is a hexamer (44,53,55,57,58,65,66,68) or pentamer (67,69,70). To resolve this conflict, it is critical to understand how the

pRNA ring is formed. The elucidation of the mechanism in pRNA ring formation reported here has provided solid evidence that a pRNA ring on the phi29 DNA-packaging motor is indeed a hexamer (Supplementary animations).

MATERIALS AND METHODS

Preparation of Cy3-labeled RNA

The 5′-end Cy3 labeling of RNA was achieved by *in vitro* transcription with T7 RNA polymerase using dsDNA templates containing the T7 class II promoter (Ø2.5) in the presence of 2 mM ADOTM F550/570 (Cy3-AMP) (71–73). Transcripts were purified by electrophoresis through a 40 cm/8% polyacrylamide/8 M urea gel, which separated the Cy3-RNA from the unlabeled RNA with a distance of 5–8 mm. RNA concentration was determined by UV/Vis spectrophotometer (Beckman DU530) at an OD 260, while Cy3 concentration was obtained by measuring the absorbance at 550 nm ($\varepsilon_{550nm} = 150\,000\,M^{-1}$). Labeling efficiency was determined as the molar concentration of Cy3 divided by the molar concentration of pRNA (44).

Gel shift assay for the binding of pRNA to connector

A final concentration of 0.5 μM purified C-strep connector (53,60,61) was mixed with different kinds of RNA, including monomeric pRNA Cd′ or tRNA, at various concentrations from 0.0625 μM to 4 μM by 2-fold increasing for 10 min. The complex was then loaded on 0.8% agarose gel in TAE buffer (40 mM Tris–HCl, 1 mM EDTA, 20 mM Acetate, pH 8.5), and the gel was run with a constant voltage of 70 V at 4°C. The gel was first stained with ethidium bromide to detect RNA and then stained by Coomassie brilliant blue (0.004% Coomassie brilliant blue in 0.5% methanol and 8.5% acetic acid) with gentle agitation at ambient temperature overnight to reveal the protein bands.

Stoichiometry determination of RNA on the procapsid/RNA complex by photobleaching assay

Sucrose gradient sedimentation was performed to separate the procapsid/5′Cy3 RNA complex from free Cy3-RNA. The complexes were prepared as previously described (44,60) and were loaded onto the top of a linear 5–20% sucrose gradient in TMS (100 mM Tris–HCl, pH 8.0, 10 mM $MgCl_2$, 100 mM NaCl) buffer. After being spun in a Beckman L-80 ultracentrifuge at 35 000 r.p.m. for 1 h at 20°C in a SW55 rotor, fractions were collected from the bottom of the tube.

The purified procapsid/RNA complex was immobilized in a flow chamber on a quartz slide by means of an anti-phi29 procapsid antibody. Photobleaching in the presence of an oxygen scavenging system (1% β-D-glucose, 10 mM β-mercaptoethanol and 1% GODCAT solution, a mixture of glucose oxidase and catalase) was carried out with a single molecule total internal reflection microscopy setup (44,72,74). Sequential images were taken with an exposure time of 200 ms. The recorded movie, with more than 1000 frames, was analyzed by Kinetic Imaging (Andor Technology, South Windsor, CT, USA). To analyze the steps of photobleaching, a circled region around the bright fluorescent spot was selected, and the average fluorescence intensity was obtained after subtracting the background intensity. Each step of decreasing fluorescence intensity represents one single Cy3 fluorophore that was attached to a single RNA. The number of photobleaching steps reveals the copy number of Cy3 RNA bound to each procapsid (44,72).

Assay for procapsid/RNA interaction by sucrose gradient sedimentation

The binding assay for procapsid/RNA interaction has been described (60). Briefly, the procapsid was incubated with varieties of [^{3}H]pRNA in the presence of Mg^{2+}. Sucrose gradient sedimentation was performed to separate the procapsid/[^{3}H]pRNA complex. The above mixtures were loaded onto the top of a linear 5–20% sucrose gradient in TMS buffer and spun in a Beckman L-80 ultracentrifuge at 35 000 r.p.m. for 30 min at 20°C in a SW55 rotor. Upon centrifugation, fractions were collected from the bottom of the tube and prepared for scintillation counting.

In vitro phi29 DNA-packaging and phi29 virion assembly

The purification of procapsids, gp16 and DNA-gp3, and the procedure for DNA packaging *in vitro* have been previously described (75). Briefly, a quantity of 10 μl 0.3 μg/μl of purified procapsids was mixed with 1 μl 100 ng/μl pRNA in TMS buffer for 30 min at R.T. Presence of Mg^{2+} in TMS buffer promotes the binding of pRNA to the procapsid. These pRNA-enriched procapsids were mixed with 3 μl reaction buffer (10 mM ATP/6 mM spermidine/3 mM β-mercaptoethanol in TMS), 100 ng DNA-gp3 and 6 μl 0.5 μg/μl DNA-packaging enzyme gp16. These mixtures were then incubated for 30 min at ambient temperature. DNA-packaging efficiency was verified by agarose gel electrophoresis using a DNase protection (76). The packaged DNA, which was protected by the procapsid, was indicated on the gel.

For *in vitro* phi29 virion assembly, 30 min after the DNA-packaging reaction, neck, tail and morphogenic proteins were added to the DNA-packaging reactions to complete the assembly of infectious virions, which were assayed by standard plaque formation.

Electron microscopy of procapsid/pRNA/nano gold complex

The preparation of pRNA attached with a single gold particle and the procedure for the imaging of procapsid/pRNA/gold complex by electronic microscopy has been described (77).

RESULTS

RNA nomenclature

To facilitate the description, we use uppercase and lowercase letters to represent the right and left interlocking hand loops, respectively, of the pRNA. Various pRNA mutations mentioned in this article with substitutions in

the right and left hand loops are listed in Table 1. The same letter in upper and lower cases, e.g. C and c′, indicates their competence to interlock based on complementary base pairing; whereas, different letters, such as C and d′, indicate noncomplementary base pairing and therefore incompetence to contact or bind to form a ring. For example, pRNA (Cd′) with right-hand loop C ($^{5'}G_{45}A_{46}C_{47}A_{48}$) and left-hand loop d′ ($^{3'}U_{85}C_{84}C_{83}G_{82}$) can interact with pRNA Dc′ with the left-hand loop c′($^{3'}C_{85}U_{84}G_{83}U_{82}$) and right-hand loop D ($^{5'}A_{45}G_{46}G_{47}C_{48}$), respectively, to form a hexameric ring (Figure 1 and Table 1). The right-hand loop C and the left-hand loop d′ in pRNA Cd′ cannot interlock, and thus cannot form a hexameric ring. Similarly, the right-hand loop D and the left loop c′ in pRNA Dc′ cannot interlock and thus cannot form a hexameric ring. However, a closed even number ring can be formed by the interlocking of C with c′ and D with d′ when Cd′ was mixed with Dc′ (Table 1). pRNA De′, Ea′ or Ab′ alone cannot interlock with itself to form a hexameric ring by analogy. However, a closed hexameric ring can be formed by mixing three pRNA molecules Be′, Ea′ and Ab′ (Table 1).

Hexameric pRNA complex was not formed prior to binding to the procapsid or connector

As reported previously, pRNAs form a hexameric ring (44,57,58,65) around the connector (53,60) of phi29 DNA-packaging motor. One intriguing question that remains to be addressed is whether the ring is formed prior or subsequent to the binding to the connector. It was found that pRNA in solution forms monomers or dimers (55,56). Formation of trimers requires a special design of interlocking loops A, b′, B, e′, E and a′ (Supplementary Figure S1, lane 6). Years of extensive investigation revealed that free hexameric pRNA could not be detected in solution in the absence of connector or procapsid (Figure 2 and Supplementary Figure S1) (55). Formation of a stable pRNA hexamer requires procapsid (or connector) as a scaffold [Figure 2A(b)]. The native PAGE gel showed pRNA Ab′ or Dc′ formed only monomers, Ab′ + Ba′ or Cd′ + Dc′ formed dimers, and Ab′ + Be′ + Ea′ formed trimers (Supplementary Figure S1). Comparison of the histograms of photobleaching steps by single molecule counting (44,72) of different pRNAs also showed that without the procapsid (or connector), pRNA alone did not form a hexamer (Figure 2B).

Individual pRNA monomer and nonspecific RNA bound to the motor with similar affinity

Gel shift assay revealed that the binding affinity of nonspecific tRNA to connector was very close to that of the individual monomeric pRNA Cd′ (Figure 3), Dc′, De′ or Ea′ (data not shown).

Data from single molecule imaging indicates that tRNA and the individual monomer of pRNA Cd′ (or other pRNA monomer without self-interlocking left or right loops) showed similar results with weaker binding to procapsid (Figure 4B and C). Quantification following our published methods (44,72) showed that both the procapsid/tRNA complex and the procapsid/pRNA Cd′ complex obtained a similar pattern in the histogram of photobleaching steps (Figure 5A and B). Photobleaching analysis further revealed that the majority of both types of complexes only contained one fluorescent RNA molecule (Figures 4G, H and 5). The validity of the 3D structure of Cd′, as well as its potential competency in group effort to drive the motor, was confirmed by the findings that: (i) when Cd′ was mixed with Dc′, they formed a pRNA dimer in the native gel (Supplementary Figure S1); (ii) unlabeled Dc′ when added to the fluorescent Cd′ demonstrated that each motor contained six pRNA (three labeled Cd′ and three unlabeled Dc′) (see subsequently and Figure 4F insert); and (iii) when Cd′ was mixed with Dc′, they were able to package phi29 genomic DNA and produced infectious virions with an optimal yield in the *in vitro* phi29 assembly system (44,72) (Figure 6).

Hexameric ring formation stabilized the connector/pRNA complex

(1) The monomeric pRNA Cd′ or Dc′ alone (incompetent to form a hexameric ring due to the lack of interlocking loops by itself) had very low binding to the procapsid (Figure 7), like the negative controls of nonspecific tRNA or DNA oligo. These data agreed with previous publications showing that 5S rRNA did not compete with pRNA binding on the procapsid (54,62). In contrast, when Dc′ was added to Cd′ (competent to form a hexameric ring), the binding of Cd′ to procapsid was greatly enhanced (Figure 7). Full activities in DNA packaging (Figure 6A) and phi29 virion assembly (Figure 6B) were regained as well. Single molecule quantification (44,72) revealed that each motor contained six pRNAs (three labeled Cd′ and three unlabeled Dc′) (Figure 4F insert). However, with either monomeric pRNA Cd′ alone or tRNA, very few RNA molecules were found to be associated with procapsids (Figure 4B and C). Furthermore, for those procapsid that did retain RNA, each procapsid contained only one RNA molecule (Figure 4G and H) (Supplementary animations).

(2) When pRNA Aa′ with two self-interlocking loops A and a′ (competent to form a hexameric ring due to the potential to develop six pairs of interlocking loops A and a′) was tested alone, it was found to be active in procapsid binding or DNA packaging (Table 1; Figure 4 and Figure 6).

(3) Individual pRNA Ab′, Be′ or Ea′ monomer, without hexameric ring forming capability, bound to the connector or procapsid poorly and was inactive in DNA-packaging or virion assembly when used alone. However, procapsid binding was enhanced, DNA was packaged and virions were produced when Ab′, Be′ and Ea′ were mixed together (Supplementary Figure S2).

(4) When one of the interlocking links in the competent group was disrupted, procapsid binding affinity of the group was substantially reduced to a level close to the nonspecific RNA. For example, when the pRNA Dc′ in a Cd′/Dc′ group was replaced by pRNA De′, its procapsid binding was weak (Figure 8). In the pRNA Ab′/Ea′ group, since the interlocking link between loop b′ and E was disrupted, the assembly activity was reduced by more

Table 1. Illustration of pRNA hexamer formation[a]

pRNA	Right |||| Left Loop sequence	Hexamer ring	Procapsid binding	DNA packaging and virion assembly
pRNA (Aa′) (Dimer with interlocking loops)	A 5′ GGAC 3′ |||| a′ 3′ CCUG 5′	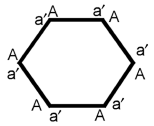	+++++	+++++
pRNA (Cd′) (Unpaired loops)	C 5′ GACA 3′ · d′ 3′ UCCG 5′	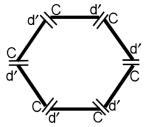	+	+
pRNA (Dc′) (Unpaired loops)	D 5′ AGGC 3′ · c′ 3′ CUGU 5′	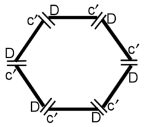	+	+
pRNA (Cd′+Dc′) (Dimer with interlocking loops)	C 5′ GACA 3′ |||| c′ 3′ CUGU 5′ D 5′ AGGC 3′ |||| d′ 3′ UCCG 5′	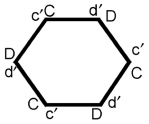	+++++	+++++
Artificial pRNA (Yy′) (Interlocking loops)	Y 5′ GAAAA 3′ ||||| y′ 3′ CUUUU 5′	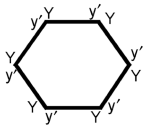	+++++	+++++
Artificial pRNA (Gg′) (Interlocking loops)	G 5′ GUUUU 3′ ||||| g′ 3′ CAAAA 5′	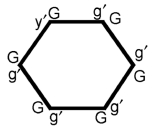	+++++	+++++
pRNA (Ab′+Ea′) (Dimer missing one link)	E 5′ GCCA 3′ ·| b′ 3′ UGCG 5′ A 5′ GGAC 3′ |||| a′ 3′ CCUG 5′	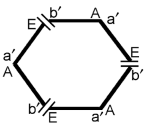	++	++
pRNA (Ab′+Be′+Ea′) (Trimer with interlocking loops)	A 5′ GGAC 3′ |||| a′ 3′ CCUG 5′ B 5′ ACGC 3′ |||| b′ 3′ UGCG 5′ E 5′ GCCA 3′ |||| e′ 3′ CGGU 5′	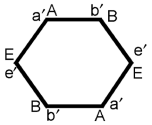	+++++	+++++
pRNA (Ab′+Bc′+Cd′) (Trimer missing one link)	A 5′ GGAC 3′ ·|| d′ 3′ UCCG 5′ B 5′ ACGC 3′ |||| b′ 3′ UGCG 5′ C 5′ GACA 3′ |||| c′ 3′ CUGU 5′	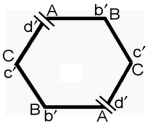	++	++

[a]'||' indicates that the loops are not paired and closed ring cannot be formed. The '+' from one to five indicates the strength of procapsid binding or phi29 virion assembly activity.

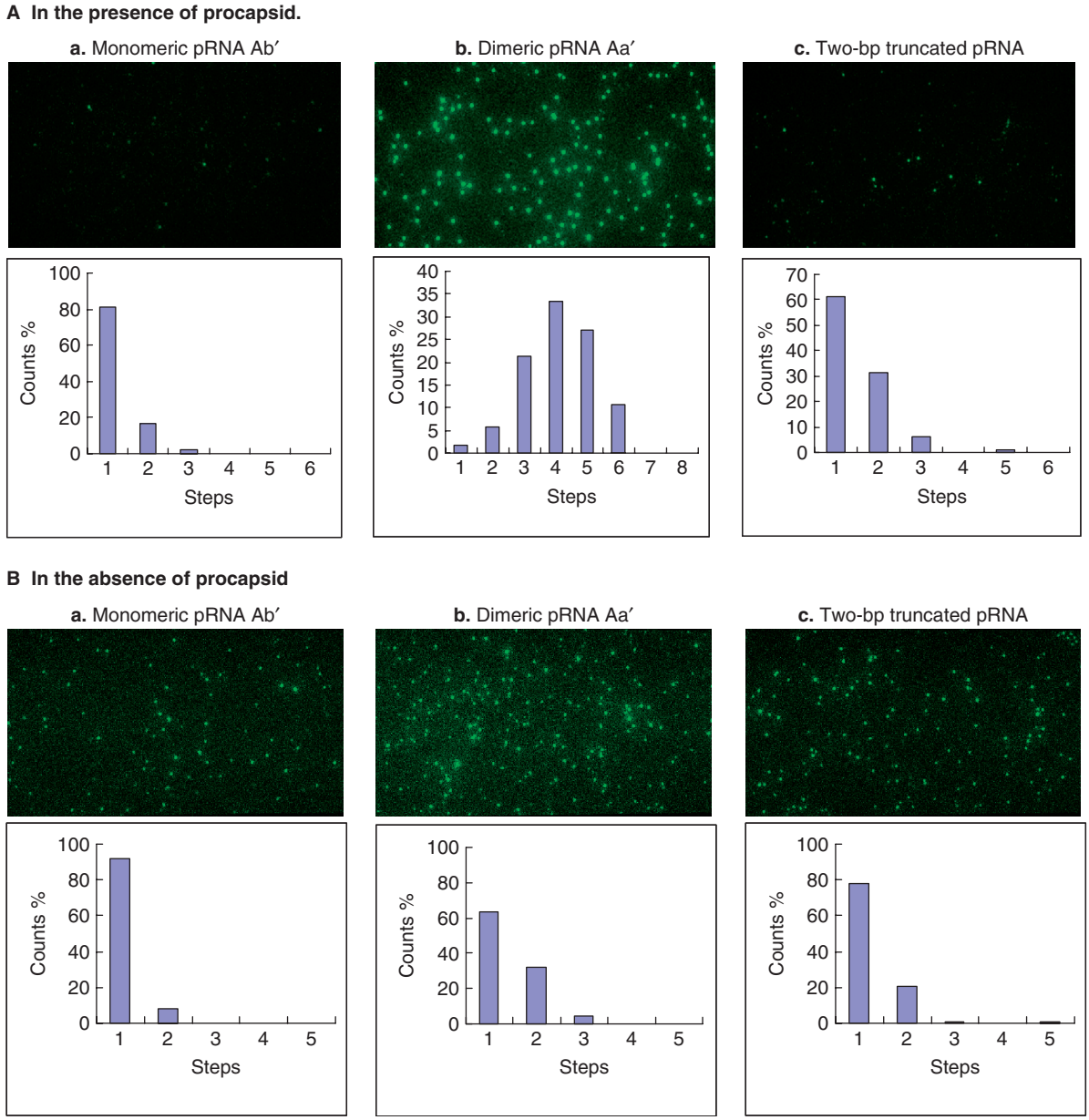

Figure 2. Single molecule imaging for the comparison of pRNA oligomerization in the presence (**A**) and in the absence (**B**) of procapsid. (a) Monomeric pRNA Ab′; (b) dimeric pRNA Aa′; and (C) pRNA with the deletion of 2-nt pairs to reduce the diameter of the hexameric ring. Each bright spot represents one single procapsid/Cy3-pRNA complex (A) or the Cy3-pRNA complex in the absence of procapsid or connector (**B**). The histogram represents the photobleaching steps of the complex that contained the Cy3-labeled RNA. The measurements and pRNA counting have been performed using the single molecule total internal reflection florescence dual view system (44,72).

than 1000-fold (Table 1). Similarly, in the group Ab′/Bc′/Cd′, the DNA-packaging activity was undetectable, and virion assembly activity was also reduced by more than 100-fold due to the disruption between the interlocking loop A and d′ (Table 1, Supplementary Figure S2).

Mutant RNAs with a 4% reduction or extension in the circumference of the ring were incompetent to bind procapsid and were inactive in DNA packaging

Phi29 connector has a truncated cone shape with both a wide end and narrow end. The wide end is embedded in the capsid while the narrow end is exposed outside (Figure 1). X-ray crystallography revealed that the connector contains three sections: a narrower section with a diameter of 6.6 nm, a central section with a diameter of 9.4 nm and a wider section with a diameter of 13.8 nm (30). The model of the 3D structure of pRNA hexamer revealed that the ring contains a central channel with a diameter of 7.6 nm that can sheathe onto the 6.6 nm narrow end of the connector and be secured by the connector's 9.4 nm central section (48) (Figure 1A). It indicates that the hexameric RNA internal channel's diameter of 7.6 nm (48) is critical to stabilize the

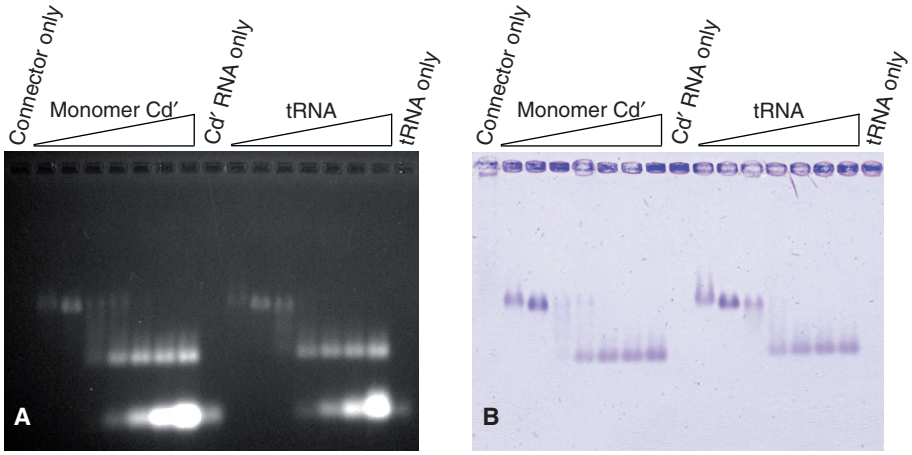

Figure 3. Agarose gel shift assay to compare the binding affinity of connector with individual pRNA monomer Cd′ or tRNA. A final concentration of 0.5 μM purified connector was mixed with an increasing concentration of pRNA monomer Cd′ or nonspecific tRNA. The triangle indicates a 2-fold increase in RNA concentration. The complex was separated by 0.8% agarose gel. The gel was first stained with ethidium bromide to detect RNA (**A**) and then stained by Coomassie brilliant blue to detect the protein (**B**).

connector/hexameric pRNA complex. It is expected that if the diameter is too small, some of the loops cannot reach each other and a hexamer cannot be formed around the connector. On the other hand, if the diameter is too large, a loose hexamer would fall off the connector, even if the hexamer had been formed. To test this hypothesis, four mutant pRNAs, with either a 2-bp truncation or insertion, were constructed. The reduction and insertion sites were located at nucleotide #33 and #89, respectively (Figure 1C). These two locations are involved in determining the diameter of the hexameric ring (48). The native gel revealed that the mutant pRNA with 2-bp truncation was competent to form dimers in solution, but not hexamers (Supplementary Figure S1, lane 7). This suggests that the mutant pRNA assumed a folding similar to the wild-type pRNA, and the mutation did not significantly change the energy required for dimer formation via the interlocking loops. However, the pRNAs predicted to form a ring with smaller diameter were incompetent in procapsid binding, DNA-packaging and phi29 virion assembly (Figure 6). This supports our assumption that the mutated pRNA did not form stable procapsid/pRNA complexes due to the reduced diameter of the predicted hexameric ring.

Hexamer is the prevalent product on the procapsid

It has been reported that when procapsids were incubated with fluorescent pRNA, which is capable of forming hexameric rings, nearly all of the fluorescent spots contained six copies of pRNA as demonstrated by single fluorescent pRNA counting and statistics (44). Here, nanogold electron microscopy was used to observe the binding of pRNA Aa′ to the procapsid. Each pRNA was labeled with one single 5-nm nanogold particle. After purification to homogeneity, the pRNA/gold complexes were incubated with procapsid and then examined by TEM. Although occasionally a procapsid with one to five golds had appeared due to incomplete labeling, it is interesting to find that we obtained an image with the procapsids containing either six gold particles representing six pRNAs or no gold particles at all (Figure 9). This finding strongly supports the conclusion that the formation of a hexamer stabilizes the procapsid/RNA interaction, and any bound pRNA fewer than six copies would detach from the procapsid if a hexameric ring was not formed. Without stabilizing by the formation of the hexamer, one or two pRNAs unstably bound to the procapsid could fall off the procapsid after transient binding.

Construction of artificial pRNAs active in DNA packaging and production of infectious phi29 virion

The aforementioned results support our hypothesis that formation of a hexameric ring strongly stabilizes the procapsid/RNA complex. To further support this conclusion, new artificial RNAs Yy′ or Gg′ with a sequence different from that of phi29 pRNA were designed and constructed to test its activities in procapsid binding and in gearing the motor in DNA packaging. These RNAs contained a right-hand loop Y or G and a left-hand loop y′ or g′ that were complementary so as to promote the formation of the hexameric ring. It also contained a helical region at the paired 5′- and 3′-ends (Supplementary Figure S3) for the binding of the DNA packaging ATPase gp16 (46,63). It is interesting to find that artificial pRNAs bound to the procapsid similar to pRNA Aa′ (compare Figure 4D and E) were fully active in DNA packaging and infectious phi29 virion production (Figure 6). Further investigation through single molecule photobleaching studies on the complex of procapsid/Cy3-artificial RNA (Yy′) revealed a six-step photobleaching (Figure 4J) (44), indicating the presence of six pRNA bound to procapsid. This finding suggests that the artificial pRNAs Yy and Gg′ were biologically similar to that of the normal phi29 pRNA (Figure 4I).

DISCUSSION

In this article, we have shown that the binding of individual pRNA to the motor connector is not sequence specific.

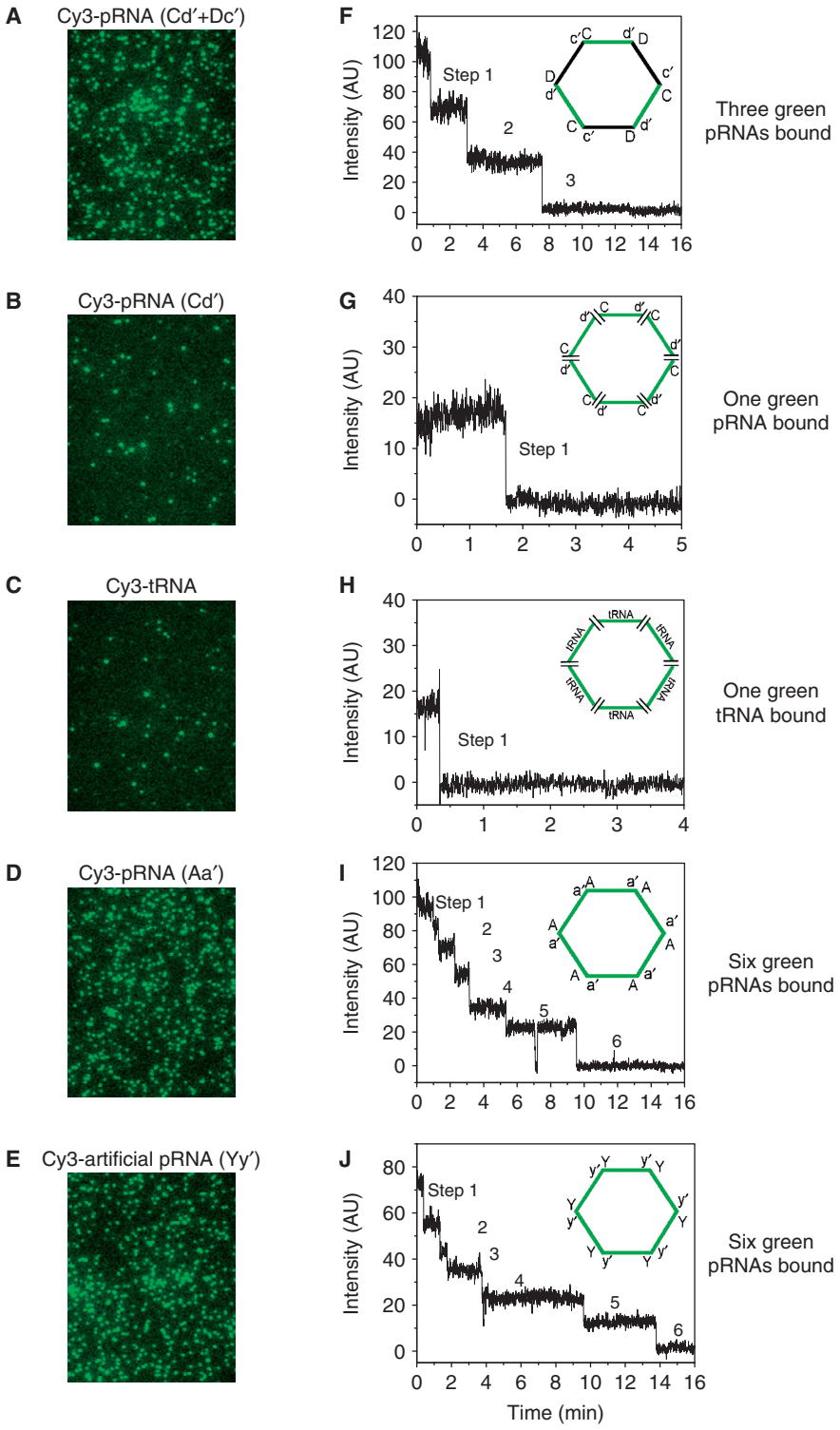

Figure 4. Single molecule counting of RNA molecules that bound to each procapsid (44,72). (**A**–**E**) Single molecule imaging of procapsid/Cy3-RNA complex. Each bright spot represents one single procapsid/Cy3-pRNA complex. Cy3 signals were presented in a pseudo color, green. (**A**) complexes of procapsid/Cy3-pRNA (Cd′ + Dc′); (**B**) procapsid/Cy3-pRNA (Cd′); (**C**) procapsid/Cy3-tRNA; (**D**) procapsid/Cy3-pRNA (Aa′); and (**E**) procapsid/Cy3-pRNA (Yy′). (**F**–**J**). Typical plot of fluorescence intensity versus time for Cy3-pRNA in procapsid/pRNA complexes. Each step in photobleaching represents the presence of one Cy3-RNA, which was labeled with a single Cy3-fluorophore. Data of photobleaching steps were obtained using methods in our recent publications (44,72). Examples of the histogram distribution are shown in Figure 5. Statistical analysis (44) revealed that the resulting data were highly significant. The '||' at the vertices of the inserted diagram indicates that two loops were noncomplementary and could not interlock to form a ring. Cy3-labeled RNA is shown as a green line, while unlabeled RNA is shown as a black line in the inserted diagram (Animations available at: http://www.eng.uc.edu/nanomedicine/newmovs.html).

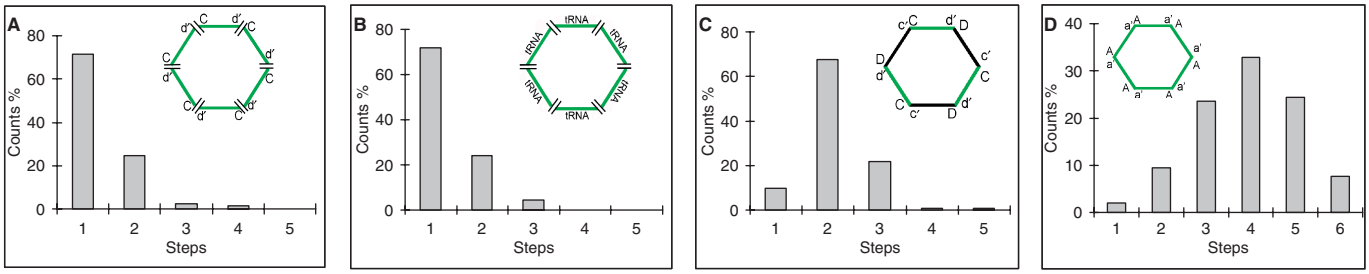

Figure 5. Histogram showing the photobleaching steps of the procapsids containing fluorescence pRNA in single molecule counting using the single molecule total internal reflection florescence dual view system (44,72) (Animations available at: http://www.eng.uc.edu/nanomedicine/newmovs.html).

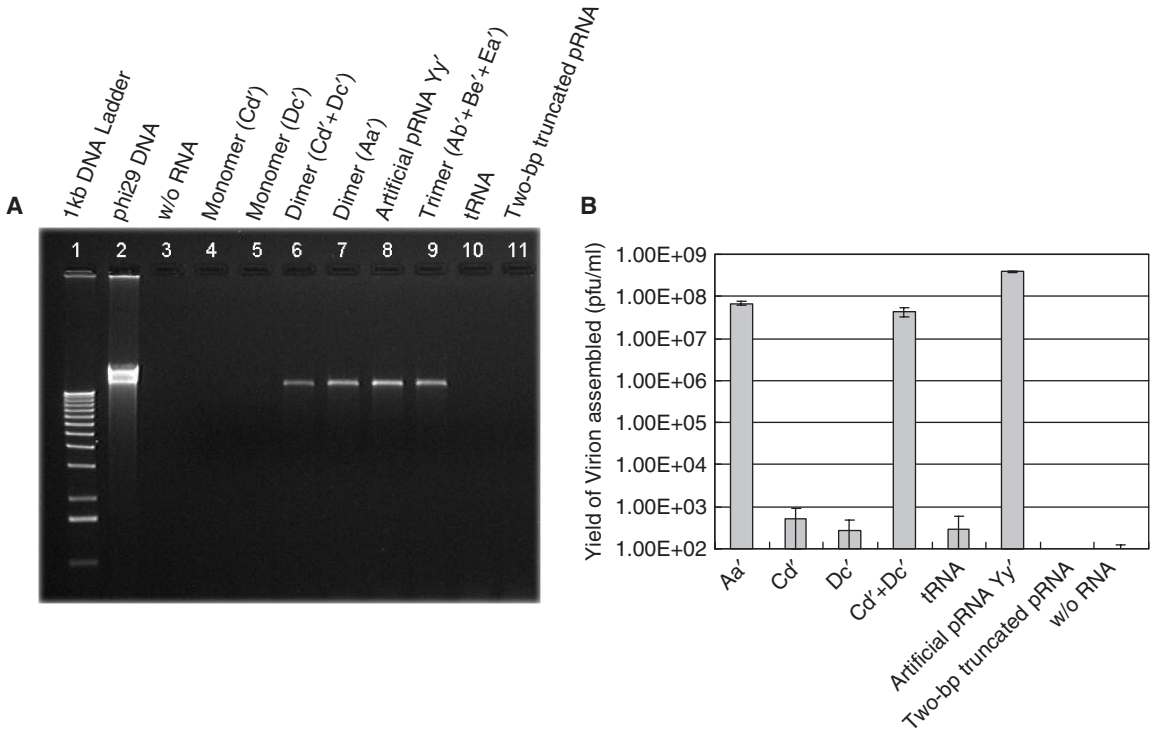

Figure 6. Comparison of the activity of DNA-packaging (**A**) and virion assembly (**B**) of different RNAs. The packaged DNA was protected from DNase I digestion and was indicated in the gel (lanes 6–9 in A). Lane 2 is the input phi29 DNA control without DNase I digestion.

Consequently what could be the mechanisms of protein/RNA interactions that resulted in the specific requirement of phi29 pRNA in procapsid binding and DNA packaging? All of the above results can be explained as follows. Each wild-type phi29 pRNA itself contains both inter- and intra-molecular interlocking loops, and are therefore able to form a closed ring via hand-in-hand interaction of those loops (56). With the Cd′/Dc′ group as an example, the individual pRNA Cd′ or Dc′ by itself has low procapsid binding affinity and could not package DNA or assemble infectious phi29 virion, since they only contain mismatched loops and cannot form a closed ring. However, the closed ring is formed to produce a hexamer containing three Cd′ and three Dc′ arranged in alternating order when Cd′ is mixed with Dc′ (Figure 4F). Thus, pRNAs bound to the procapsid firmly and DNA was packaged to produce infectious virions. In contrast, interruption of any one of the interlocking links could impede the formation of the hexameric ring, resulting in an incompetence of the pRNA group to bind to the connector. Extension or reduction of the circumference of the ring resulted in no motor binding. Furthermore, a ring with three 2-bp deleted pRNAs and three 2-bp lengthened pRNA is functional in DNA-packaging and virion assembly (Shu and Guo, manuscript in preparation). It confirmed that the specificity in procapsid/pRNA interaction is attributed to the formation of the static ring that surrounds the connector. All individual RNA subunits, no matter if they are pRNA, nonspecific tRNA, were competent to bind to the three basic residues, Arg–Lys–Arg, at the N-terminus of the connector protein gp10, which protrudes out of the procapsid (53,60). A dynamic and low affinity interaction between RNA and the connector could make some of the RNAs fall off the connector if the ring was not formed. However, forming a static hexameric ring via the interlocking loops and sheathing around the connector

strongly stabilizes the procapsid/RNA complex, which also keeps the RNA bound to both the connector the procapsid. (Supplementary animations)

Phi29 DNA-packaging motor is geared by a pRNA ring, of which the stoichiometry is under fervent debate. Phage DNA-packaging motor contains a 6-fold (12-subunit) connector surrounded by a 5-fold symmetrical capsid shell (26). The presence of pRNA hexamer and the inter-pRNA interaction of the suppressor mutants were demonstrated by extensive complementation analyses in 1997 (65). In 1998, two labs (57,58) independently reported that pRNA forms hexamers as a part of the phi29 motor.

Subsequent to the biochemical, mathematical and genetic approaches to find the hexamer, a hexameric pRNA ring was reported in 2000 using Cryo-electron microscopy (Cryo-EM) (68). In contrast, the cryo-EM approach by others resulted in a pRNA pentamer (67,69,70). Cryo-EM image reconstruction for RNA remains challenging due to the sensitivity of RNA to RNase degradation during sample preparation, as well as the structural flexibility resulting from the presence of multiple free energy levels of folding for RNA. The underestimation of the copy number of RNA per procapsid caused by RNase degradation has also been observed in the single molecule photobleaching studies. The results from these studies demonstrated that five-steps occur more often than six-steps, even though the pRNA ring was explicitly determined to be a hexamer (44). In addition, those who support the hexamer and those who support the pentamer hold different points of view. The hexamer supporters argued that pRNA binds to the connector, which contains 12 subunits and holds 6-fold symmetry. The pentamer supporters claimed that pRNA binds to the procapsid shell, which shows a 5-fold symmetry (69). However, cross-linking approaches revealed that pRNA did not bind to the procapsid protein, but to the connector (49). Xiao *et al.* (60) has provided solid evidence that pRNA binds to the N-terminus of the connector protein gp10. Further analysis reveals that the three basic amino acids, Arg–Lys–Arg, at the N-terminus of the gp10 are responsible for pRNA binding. Mutation of any two of these three amino acids resulted in complete abolishment of pRNA binding to the DNA-packaging motor (53,61). Recent single molecule counting, using high sensitive dual view total internal reflection fluorescence microscopy with photobleaching technology, revealed that each DNA-packaging motor contains six

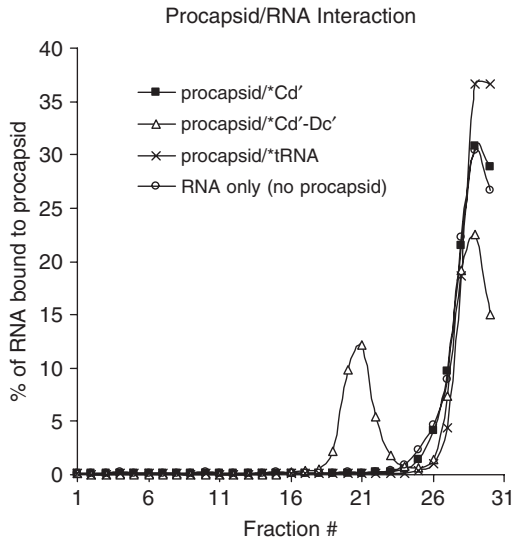

Figure 7. Sucrose gradient sedimentation to compare the binding efficiency of pRNA and tRNA to procapsid. The [^{3}H] pRNA Cd′ (black square), [^{3}H] Cd′ + Dc′ (open triangle) and tRNA (asterisk) (2.5 pmol each) were incubated with procapsid and then subjected to 5–20% sucrose gradient sedimentation.

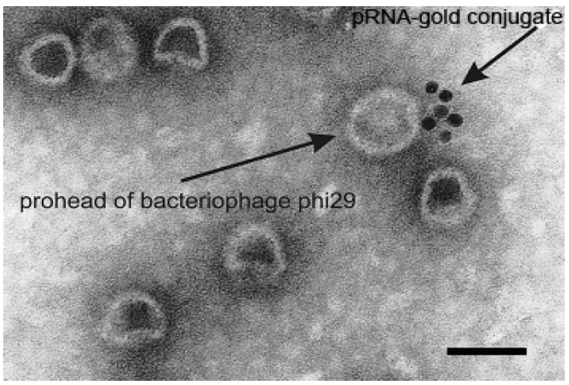

Figure 9. Transmission electron micrographs of phi29 procapsids/pRNA-gold complexes. Bar = 50 nm.

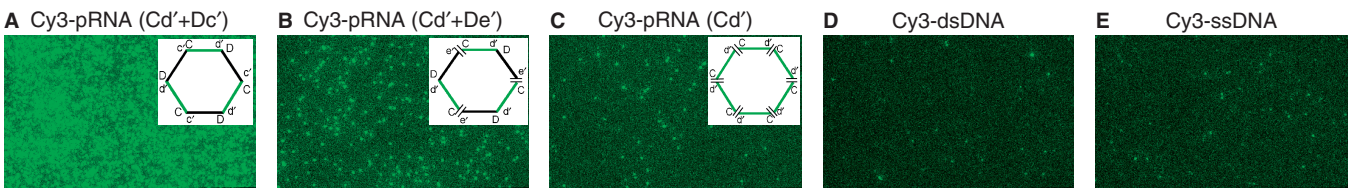

Figure 8. Single molecule imaging to compare the procapsid-binding efficiency between the ring forming pRNA group (**A**) and the pRNA group with one of the interlocking links disrupted (**B**). The binding of procapsid with pRNA monomer Cd′ (**C**), dsDNA (**D**) and ssDNA (**E**) were also shown as controls. The pRNA Cd′ was labeled with a single Cy3 molecule. Cy3-ssDNA was synthesized by IDT. The procapsid/Cy3-RNA or procapsid/Cy3-DNA complex, which was purified from 5–20% sucrose gradient and attached to the quartz slide surface coated with anti-phi29 procapsid antibody. (A) Procapsid/Cy3-pRNA(Cd′ + Dc′); (B) procapsid/Cy3-pRNA(Cd′ + De′) with one link disrupted; (C) procapsid/Cy3-pRNA(Cd); (D) procapsid/Cy3-dsDNA; and (E) procapsid/Cy3-ssDNA.

copies of pRNA (44). The group who asserted the pentameric pRNA ring argued that pRNA hexamers are formed initially, but after binding, one of the pRNAs dissociates from the procapsids due to a conformational change, leaving five pRNAs still bound (67,69,70). However, single molecule fluorescence microscopy studies of purified DNA-packaging intermediates revealed that the active motor still contained six copies of pRNA during DNA translocation (44).

The results in this article support our earlier findings using pRNA with interlocking loops. Previously, it was reported that only the hexameric pRNA ring was active in DNA packaging (44,57,65). Mixing two inactive pRNAs, such as pRNA Cd′ and Dc′ in a 1:1 molar ratio, resulted in full production of infectious virions, indicating that the stoichiometry of the pRNA should be a multiple of two. Three inactive pRNAs, Ab′, Be′ and Ea′, which become fully active when mixed together, suggest that the number of pRNAs in the DNA-packaging complex is a multiple of three. The common multiple of two and three is six. It was found that purified pRNA trimers have the highest specific activity (78) compared with the pRNA dimer and monomer. It would be astonishing if two trimers could form a pentamer. Single molecule imaging in this report revealed that the ring was formed by either a pure dimer or by pure trimer alone. Again, these data strongly support the argument that the ring is a common multiple of two and three, which must be a hexamer. These data also suggest that the pRNA ring contains an even number of pRNA, since the purified pRNA dimer was the building block of the ring. It was impossible to build a 5-member ring when pure dimers or pure trimers were used alone. It is not easy to account for how a pentamer could be formed from an even number of binding units (pRNA dimer) on a targeted base with even-numbered symmetry (the dodecameric connector). The finding of hexamer was also supported by a DNA-packaging model proposed by Fang *et al*. (66).

Natural DNA or RNA translocation motors contain components that mostly display a hexameric configuration for contacting DNA or RNA, as do the large AAA+ family (the ATPases associated with a variety of cellular activities), to which phi29 DNA-packaging protein gp16 belongs (79,80). The formation of a hexameric ring indicates that this class of nanomachines might possess a similar mechanism in nucleotide contact or DNA/RNA translocation. DNA polymerase (81), P4 RNA packaging motor (3), RNA polymerase (9), helicase (2,82), Rho (83,84), DNA polymerase processivity factor (85), BPV E1 replication initiator (86,87) and tens of other nucleotide/nucleic acids binding or translocating proteins all exist as hexamer (2,5,10–14,88–90). Convincing data have revealed that the pRNA ring on the phi29 motor was a hexamer. It would be very interesting to find out why a hexamer was quantified into a pentamer by cryo-EM. We do not exclude the possibility that there may be novel features of the pRNA and this motor organization that, if identified in the future, will explain the discrepancy in the findings regarding hexamer and pentamer.

SUPPLEMENTARY DATA

Supplementary Data are available at NAR Online.

ACKNOWLEDGEMENTS

We thank Wulf-Dieter Moll for preparation of the EM image of the procapsid/pRNA-gold complex; Nick Snead and Stephen Perrin II for construction of the pRNA with truncation or deletions; Faqing Huang and Dan Shu for their technical assistance as well as valuable comments; Jia Geng and Robert B. Deutsch for their assistance in making the animation; Lynn Enquist and Ian Molineux for their insightful comments on the manuscript.

FUNDING

Supported by National Institutes of Health grant (R01-GM59944, EB003730); and PN2 EY018230 from NIH Nanomedicine Development Center for Phi29 DNA Packaging Motor for Nanomedicine through NIH Roadmap for Medical Research. Funding for open access charge: National Institutes of Health grant R01-GM59944.

Conflict of interest statement. P.G. is the co-founder of Kylin Therapeutics Inc.

REFERENCES

1. Enemark,E.J. and Joshua-Tor,L. (2006) Mechanism of DNA translocation in a replicative hexameric helicase. *Nature*, **442**, 270–275.
2. West,S.C. (1996) DNA helicases: new breeds of translocating motors and molecular pumps. *Cell*, **86**, 177–180.
3. Kainov,D.E., Mancini,E.J., Telenius,J., Lisai,J., Grimes,J.M., Bamford,D.H., Stuart,D.I. and Tuma,R. (2008) Structural basis of mechanochemical coupling in a hexameric molecular motor. *J. Biol. Chem*., **283**, 3607–3617.
4. Ciampi,M.S. (2006) Rho-dependent terminators and transcription termination. *Microbiology*, **152**, 2515–2528.
5. Geiselmann,J., Wang,Y., Seifried,S.E. and von Hippel,P.H. (1993) A physical model for the translocation and helicase activities of *Escherichia coli* transcription termination protein rho. *Proc. Natl Acad. Sci. USA*, **90**, 7754–7758.
6. Mayanagi,K., Miyata,T., Oyama,T., Ishino,Y. and Morikawa,K. (2001) Three-dimensional electron microscopy of the clamp loader small subunit from Pyrococcus furiosus. *J. Struct. Biol*., **134**, 35–45.
7. VanLoock,M.S., Alexandrov,A., Yu,X., Cozzarelli,N.R. and Egelman,E.H. (2002) SV40 large T antigen hexamer structure: domain organization and DNA-induced conformational changes. *Curr. Biol*., **12**, 472–476.
8. Jeruzalmi,D., O'Donnell,M. and Kuriyan,J. (2002) Clamp loaders and sliding clamps. *Curr. Opin. Struct. Biol*., **12**, 217–224.
9. Cramer,P., Bushnell,D.A. and Kornberg,R.D. (2001) Structural basis of transcription: RNA polymerase II at 2.8 angstrom resolution. *Science*, **292**, 1863–1876.
10. Martin,A., Baker,T.A. and Sauer,R.T. (2005) Rebuilt AAA + motors reveal operating principles for ATP-fuelled machines. *Nature*, **437**, 1115–1120.
11. Hanson,P.I. and Whiteheart,S.W. (2005) AAA+proteins: have engine, will work. *Nat. Rev. Mol. Cell. Biol*., **6**, 519–529.
12. Hishida,T., Han,Y.W., Fujimoto,S., Iwasaki,H. and Shinagawa,H. (2004) Direct evidence that a conserved arginine in RuvB AAA(+) ATPase acts as an allosteric effector for the ATPase activity of the adjacent subunit in a hexamer. *Proc. Natl Acad. Sci. USA*, **101**, 9573–9577.

13. Willows,R.D., Hansson,A., Birch,D., Al-Karadaghi,S. and Hansson,M. (2004) EM single particle analysis of the ATP-dependent BchI complex of magnesium chelatase: an AAA(+) hexamer. *J. Struct. Biol.*, **146**, 227–233.
14. Aker,J., Hesselink,R., Engel,R., Karlova,R., Borst,J.W., Visser,A.J.W.G. and de Vries,S.C. (2007) *In vivo* hexamerization and characterization of the Arabidopsis AAA ATPase CDC48A complex using forster resonance energy transfer-fluorescence lifetime imaging microscopy and fluorescence correlation spectroscopy. *Plant Physiol.*, **145**, 339–350.
15. Brion,P. and Westhof,E. (1997) Hierarchy and dynamics of RNA folding. *Ann. Rev. Biophys. Biomol. Struct.*, **26**, 113–137.
16. Pan,T., Long,D.M. and Uhlenbeck,O.C. (1993) Divalent metal ions in RNA folding and catalysis. In Gesteland,R.F. and Atkins,J.F. (eds), *RNA World*, Cold Spring Harbor Laboratory Press, Cold Spring Harbor, NY, pp. 271–302.
17. Bernacchi,S., Freisz,S., Maechling,C., Spiess,B., Marquet,R., Dumas,P. and Ennifar,E. (2007) Aminoglycoside binding to the HIV-1 RNA dimerization initiation site: thermodynamics and effect on the kissing-loop to duplex conversion. *Nucleic Acids Res.*, **35**, 7128–7139.
18. Guerrier-Takada,C., Gardiner,K., Marsh,T., Pace,N. and Altman,S. (1983) The RNA moiety of ribonuclease P is the catalytic subunit of the enzyme. *Cell*, **35**, 849–857.
19. Sarver,N., Cantin,E.M., Chang,P.S., Zaia,J.A., Ladne,P.A., Stephens,D.A. and Rossi,J.J. (1990) Ribozymes as potential anti-HIV-1 therapeutic agents. *Science*, **247**, 1222–1225.
20. Kruger,K., Grabowski,P.J., Zaug,A.J., Sands,J., Gottschling,D.E. and Cech,T.R. (1982) Self-splicing RNA: autoexcision and autocyclization of the ribosomal RNA intervening sequence of Tetrahymena. *Cell*, **31**, 147–157.
21. Leulliot,N. and Varani,G. (2001) Current topics in RNA-protein recognition: control of specificity and biological function through induced fit and conformational capture. *Biochemistry*, **40**, 7947–7956.
22. Williamson,J.R. (2000) Induced fit in RNA-protein recognition. *Nat. Struct. Biol.*, **7**, 834–837.
23. Catalano,C.E., Cue,D. and Feiss,M. (1995) Virus DNA packaging: the strategy used by phage lambda. *Mol. Microbiol.*, **16**, 1075–1086.
24. Molineux,I.J. (2001) No syringes please, ejection of phage T7 DNA from the virion is enzyme driven. *Mol. Microbiol.*, **40**, 1–8.
25. Conway,J.F., Wikoff,W.R., Cheng,N., Duda,R.L., Hendrix,R.W., Johnson,J.E. and Steven,A.C. (2001) Virus maturation involving large subunit rotations and local refolding. *Science*, **292**, 744–748.
26. Hendrix,R.W. (1978) Symmetry mismatch and DNA packaging in large bacteriophages. *Proc. Natl Acad. Sci. USA*, **75**, 4779–4783.
27. Johnson,J.E. and Chiu,W. (2007) DNA packaging and delivery machines in tailed bacteriophages. *Curr. Opin. Struct. Biol.*, **17**, 237–243.
28. Guo,P.X. and Lee,T.J. (2007) Viral nanomotors for packaging of dsDNA and dsRNA. *Mol. Microbiol.*, **64**, 886–903.
29. Guasch,A., Pous,J., Ibarra,B., Gomis-Ruth,F.X., Valpuesta,J.M., Sousa,N., Carrascosa,J.L. and Coll,M. (2002) Detailed architecture of a DNA translocating machine: the high- resolution structure of the bacteriophage phi29 connector particle. *J. Mol. Biol.*, **315**, 663–676.
30. Simpson,A.A., Leiman,P.G., Tao,Y., He,Y., Badasso,M.O., Jardine,P.J., Anderson,D.L. and Rossman,M.G. (2001) Structure determination of the head-tail connector of bacteriophage phi29. *Acta Cryst.*, **D57**, 1260–1269.
31. Lander,G.C., Tang,L., Casjens,S.R., Gilcrease,E.B., Prevelige,P., Poliakov,A., Potter,C.S., Carragher,B. and Johnson,J.E. (2006) The structure of an infectious P22 virion shows the signal for headful DNA packaging. *Science*, **312**, 1791–1795.
32. Lebedev,A.A., Krause,M.H., Isidro,A.L., Vagin,A.A., Orlova,E.V., Turner,J., Dodson,E.J., Tavares,P. and Antson,A.A. (2007) Structural framework for DNA translocation via the viral portal protein. *EMBO J.*, **26**, 1984–1994.
33. Baumann,R.G., Mullaney,J. and Black,L.W. (2006) Portal fusion protein constraints on function in DNA packaging of bacteriophage T4. *Mol. Microbiol.*, **61**, 16–32.
34. Guo,P., Peterson,C. and Anderson,D. (1987) Prohead and DNA-gp3-dependent ATPase activity of the DNA packaging protein gp16 of bacteriophage phi29. *J. Mol. Biol.*, **197**, 229–236.
35. Hang,J.Q., Tack,B.F. and Feiss,M. (2000) ATPase center of bacteriophage lambda terminase involved in post- cleavage stages of DNA packaging: identification of ATP-interactive amino acids. *J. Mol. Biol.*, **302**, 777–795.
36. Higgins,R.R., Lucko,H.J. and Becker,A. (1988) Mechanism of *cos* DNA cleavage by bacteriophage lambda terminase-multiple roles of ATP. *Cell*, **54**, 765–775.
37. Hwang,J.S. and Bogner,E. (2002) ATPase activity of the terminase subunit pUL56 of human cytomegalovirus. *J. Biol. Chem.*, **277**, 6943–6948.
38. Gual,A., Camacho,A.G. and Alonso,J.C. (2000) Functional analysis of the terminase large subunit, G2P, of Bacillus subtilis bacteriophage SPP1. *J. Biol. Chem.*, **275**, 35311–35319.
39. Lisal,J., Kainov,D.E., Bamford,D.H., Thomas,G.J. Jr. and Tuma,R. (2004) Enzymatic mechanism of RNA translocation in double-stranded RNA bacteriophages. *J. Biol. Chem.*, **279**, 1343–1350.
40. Manne,V.S., Rao,V.B. and Black,L.W. (1982) A bacteriophage T4 DNA packaging related DNA-dependent ATPase-endonuclease. *J. Biol. Chem.*, **257**, 13223–13232.
41. Lee,T.J., Zhang,H., Liang,D. and Guo,P. (2008) Strand and nucleotide-dependent ATPase activity of gp16 of bacterial virus phi29 DNA packaging motor. *Virology*, **380**, 69–74.
42. Trottier,M. and Guo,P. (1997) Approaches to determine stoichiometry of viral assembly components. *J. Virol.*, **71**, 487–494.
43. Guo,P., Erickson,S. and Anderson,D. (1987) A small viral RNA is required for *in vitro* packaging of bacteriophage phi29 DNA. *Science*, **236**, 690–694.
44. Shu,D., Zhang,H., Jin,J. and Guo,P. (2007) Counting of six pRNAs of phi29 DNA-packaging motor with customized single molecule dual-view system. *EMBO J.*, **26**, 527–537.
45. Guo,P. (2002) Structure and function of phi29 hexameric RNA that drive viral DNA packaging motor: review. *Prog. in Nucl. Acid Res. & Mole. Biol.*, **72**, 415–472.
46. Lee,T.J. and Guo,P. (2006) Interaction of gp16 with pRNA and DNA for genome packaging by the motor of bacterial virus phi29. *J. Mol. Biol.*, **356**, 589–599.
47. Reid,R.J.D., Bodley,J.W. and Anderson,D. (1994) Characterization of the prohead-pRNA interaction of bacteriophage phi29. *J. Biol. Chem.*, **269**, 5157–5162.
48. Hoeprich,S. and Guo,P. (2002) Computer modeling of three-dimensional structure of DNA-packaging RNA(pRNA) monomer, dimer, and hexamer of phi29 DNA Packaging motor. *J. Biol. Chem.*, **277**, 20794–20803.
49. Garver,K. and Guo,P. (1997) Boundary of pRNA functional domains and minimum pRNA sequence requirement for specific connector binding and DNA packaging of phage phi29. *RNA*, **3**, 1068–1079.
50. Trottier,M., Mat-Arip,Y., Zhang,C., Chen,C., Sheng,S., Shao,Z. and Guo,P. (2000) Probing the structure of monomers and dimers of the bacterial virus phi29 hexamer RNA complex by chemical modification. *RNA*, **6**, 1257–1266.
51. Mat-Arip,Y., Garver,K., Chen,C., Sheng,S., Shao,Z. and Guo,P. (2001) Three-dimensional interaction of phi29 pRNA dimer probed by chemical modification interference, cryo-AFM, and cross-linking. *J. Biol. Chem.*, **276**, 32575–32584.
52. Zhang,C.L., Tellinghuisen,T. and Guo,P. (1997) Use of circular permutation to assess six bulges and four loops of DNA-Packaging pRNA of bacteriophage phi29. *RNA*, **3**, 315–322.
53. Atz,R., Ma,S., Gao,J., Anderson,D.L. and Grimes,S. (2007) Alanine Scanning and Fe-BABE Probing of the Bacteriophage phi29 Prohead RNA-Connector Interaction. *J. Mol. Biol.*, **369**, 239–248.
54. Trottier,M., Zhang,C.L. and Guo,P. (1996) Complete inhibition of virion assembly *in vivo* with mutant pRNA essential for phage phi29 DNA packaging. *J. Virol.*, **70**, 55–61.
55. Chen,C., Sheng,S., Shao,Z. and Guo,P. (2000) A dimer as a building block in assembling RNA: a hexamer that gears bacterial virus phi29 DNA-translocating machinery. *J. Biol. Chem.*, **275**, 17510–17516.
56. Chen,C., Zhang,C. and Guo,P. (1999) Sequence requirement for hand-in-hand interaction in formation of pRNA dimers and hexamers to gear phi29 DNA translocation motor. *RNA*, **5**, 805–818.

57. Guo,P., Zhang,C., Chen,C., Trottier,M. and Garver,K. (1998) Inter-RNA interaction of phage phi29 pRNA to form a hexameric complex for viral DNA transportation. *Mol. Cell.*, **2**, 149–155.
58. Zhang,F., Lemieux,S., Wu,X., St-Arnaud,S., McMurray,C.T., Major,F. and Anderson,D. (1998) Function of hexameric RNA in packaging of bacteriophage phi29 DNA in vitro. *Mol. Cell.*, **2**, 141–147.
59. Reid,R.J.D., Bodley,J.W. and Anderson,D. (1994) Identification of bacteriophage phi29 prohead RNA (pRNA) domains necessary for *in vitro* DNA-gp3 packaging. *J. Biol. Chem.*, **269**, 9084–9089.
60. Xiao,F., Moll,D., Guo,S. and Guo,P. (2005) Binding of pRNA to the N-terminal 14 amino acids of connector protein of bacterial phage phi29. *Nucleic Acids Res.*, **33**, 2640–2649.
61. Cai,Y., Xiao,F. and Guo,P. (2008) N- or C-terminal alterations of motor protein gp10 of bacterial virus phi29 on procapsid assembly, pRNA binding and DNA packaging. *Nanomedicine*, **4**, 8–18.
62. Reid,R.J.D., Zhang,F., Benson,S. and Anderson,D. (1994) Probing the structure of bacteriophage phi29 prohead RNA with specific mutations. *J. Biol. Chem.*, **269**, 18656–18661.
63. Zhang,C.L., Lee,C.-S. and Guo,P. (1994) The proximate 5′ and 3′ ends of the 120-base viral RNA (pRNA) are crucial for the packaging of bacteriophage ϕ29 DNA. *Virology*, **201**, 77–85.
64. Wichitwechkarn,J., Darrin Johnson and Dwight Anderson. (1992) Mutant prohead RNAs *in Vitro* packaging of bacteriophage phi29 DNA-gp3. *Mol. Biol.*, **223**, 991–998.
65. Chen,C. and Guo,P. (1997) Sequential action of six virus-encoded DNA-packaging RNAs during phage phi29 genomic DNA translocation. *J. Virol.*, **71**, 3864–3871.
66. Fang,Y., Shu,D., Xiao,F., Guo,P. and Qin,P.Z. (2008) Modular assembly of chimeric phi29 packaging RNAs that support DNA packaging. *Biochem. Biophys. Res. Commun.*, **372**, 589–594.
67. Morais,M.C., Tao,Y., Olson,N.H., Grimes,S., Jardine,P.J., Anderson,D.L., Baker,T.S. and Rossmann,M.G. (2001) Cryoelectron-microscopy image reconstruction of symmetry mismatches in bacteriophage phi29. *J. Struct. Biol.*, **135**, 38–46.
68. Ibarra,B., Caston,J.R., Llorca,O., Valle,M., Valpuesta,J.M. and Carrascosa,J.L. (2000) Topology of the components of the DNA packaging machinery in the phage phi29 prohead. *J. Mol. Biol.*, **298**, 807–815.
69. Simpson,A.A., Tao,Y., Leiman,P.G., Badasso,M.O., He,Y., Jardine,P.J., Olson,N.H., Morais,M.C., Grimes,S., Anderson,D.L. *et al.* (2000) Structure of the bacteriophage phi29 DNA packaging motor. *Nature*, **408**, 745–750.
70. Morais,M.C., Koti,J.S., Bowman,V.D., Reyes-Aldrete,E., Anderson,D and Rossman,M.G. (2008) Defining molecular and domain boundaries in the bacteriophage phi29 DNA packaging motor. *Structure*, **16**, 1267–1274.
71. Huang,F., Wang,G., Coleman,T. and Li,N. (2003) Synthesis of adenosine derivatives as transcription initiators and preparation of 5′ fluorescein- and biotin-labeled RNA through one-step *in vitro* transcription. *RNA*, **9**, 1562–1570.
72. Zhang,H., Shu,D., Huang,F. and Guo,P. (2007) Instrumentation and metrology for single RNA counting in biological complexes or nanoparticles by a single molecule dual-view system. *RNA*, **13**, 1793–1802.
73. Milligan,J.F., Groebe,D.R., Witherell,G.W. and Uhlenbeck,O.C. (1987) Oligoribonucleotide synthesis using T7 RNA polymerase and synthetic DNA templates. *Nucleic Acids Res.*, **15**, 8783–8798.
74. Ha,T., Rasnik,I., Cheng,W., Babcock,H.P., Gauss,G.H., Lohman,T.M. and Chu,S. (2002) Initiation and re-initiation of DNA unwinding by the Escherichia coli Rep helicase. *Nature*, **419**, 638–641.
75. Lee,C.S. and Guo,P. (1994) A highly sensitive system for the *in vitro* assembly of bacteriophage phi29 of *Bacillus subtilis*. *Virology*, **202**, 1039–1042.
76. Guo,P., Rajogopal,B., Anderson,D., Erickson,S. and Lee,C.-S. (1991) sRNA of bacteriophage phi29 of *B.subtilis* mediates DNA packaging of phi29 proheads assembled in *E. coli*. *Virology*, **185**, 395–400.
77. Moll,D. and Guo,P. (2007) Grouping of ferritin and gold nanoparticles conjugated to pRNA of the phage phi29 DNA-packaging motor. *J. Nanosci. Nanotech.*, **7**, 3257–3267.
78. Shu,D., Huang,L. and Guo,P. (2003) A simple mathematical formula for stoichiometry quantitation of viral and nanobiological assemblage using slopes of log/log plot curves. *J. Virol. Meth.*, **115**, 19–30.
79. Iyer,L.M., Makarova,K.S., Koonin,E.V. and Aravind,L. (2004) Comparative genomics of the FtsK-HerA superfamily of pumping ATPases: implications for the origins of chromosome segregation, cell division and viral capsid packaging. *Nucleic Acids Res.*, **32**, 5260–5279.
80. Burroughs,A.M., Iyer,L.M. and Aravind,L. (2007) Comparative genomics and evolutionary trajectories of viral ATP dependent DNA-packaging systems. In Volff,J.-N. (ed.), *Gene and Protein Evolution. Genome Dyn.*, Karger, Basel, Vol. 3, pp. 48–65.
81. Song,M.S., Dallmann,H.G. and McHenry,C.S. (2001) Carboxyl-terminal Domain III of the delta ' Subunit of the DNA Polymerase III Holoenzyme Binds delta. *J. Biol. Chem.*, **276**, 40668–40679.
82. Niedenzu,T., Roleke,D., Bains,G., Scherzinger,E. and Saenger,W. (2001) Crystal structure of the hexameric replicative helicase RepA of plasmid RSF1010. *J. Mol. Biol.*, **306**, 479–487.
83. Gogol,E.P., Seifried,S.E. and von Hippel,P.H. (1991) Structure and assembly of the Escherichia coli transcription termination factor rho and its interaction with RNA. Cryoelectron microscopic studies. *J. Mol. Biol.*, **221**, 1127–1138.
84. Burgess,B.R. and Richardson,J.P. (2001) RNA passes through the hole of the protein hexamer in the complex with the Escherichia coli Rho factor. *J. Biol. Chem.*, **276**, 4182–4189.
85. Bowers,J., Tran,P.T., Joshi,A., Liskay,R.M. and Alani,E. (2001) MSH-MLH complexes formed at a DNA mismatch are disrupted by the PCNA sliding clamp. *J. Mol. Biol.*, **306**, 957–968.
86. Sedman,J. and Stenlund,A. (1998) The papillomavirus E1 protein forms a DNA-dependent hexameric complex with ATPase and DNA helicase activities. *J. Virol.*, **72**, 6893–6897.
87. Castella,S., Burgin,D. and Sanders,C.M. (2006) Role of ATP hydrolysis in the DNA translocase activity of the bovine papillomavirus (BPV-1) E1 helicase. *Nucleic Acids Res.*, **34**, 3731–3741.
88. Geiduschek,E.P. (1997) Riding the (mono)rails: the structure of catenated DNA-tracking proteins. *Chem. & Biol.*, **2**, 123–125.
89. Young,M.C., Schultz,D.E., Ring,D. and von Hippel,P.H. (1994) Kinetic parameters of the translocation of bacteriophage T4 gene 41 protein helicase on single-stranded DNA. *J. Mol. Biol.*, **235**, 1447–1458.
90. Herendeen,D.R., Kassavetis,G.A. and Geiduschek,E.P. (1992) A transcriptional enhancer whose function imposes a requirement that proteins track along DNA. *Science*, **256**, 1298–1303.